Feature-enriched core percolation in multiplex networks

Yilun Shang
Department of Computer and Information Sciences, Northumbria University, Newcastle upon Tyne NE1 8ST, United Kingdom

(Received 24 May 2022; revised 5 November 2022; accepted 15 November 2022; published 29 November 2022)

Percolation models have long served as a paradigm for unraveling the structure and resilience of complex systems comprising interconnected nodes. In many real networks, nodes are identified by not only their connections but nontopological metadata such as age and gender in social systems, geographical location in infrastructure networks, and component contents in biochemical networks. However, there is little known regarding how the nontopological features influence network structures under percolation processes. In this paper we introduce a feature-enriched core percolation framework using a generic multiplex network approach. We thereby analytically determine the corona cluster, size, and number of edges of the feature-enriched cores. We find a hybrid percolation transition combining a jump and a square root singularity at the critical points in both the network connectivity and the feature space. Integrating the degree-feature distribution with the Farlie-Gumbel-Morgenstern copula, we show the existence of continuous and discrete percolation transitions for feature-enriched cores at critical correlation levels. The inner and outer cores are found to undergo distinct phase transitions under the feature-enriched percolation, all limited by a characteristic curve of the feature distribution.

DOI: 10.1103/PhysRevE.106.054314

I. INTRODUCTION

Percolation theory on networks provides an effective way to uncover many important structural and functional properties of diverse complex systems [1]. The pruning process involved in percolation removes nodes and edges progressively from the network according to some rule. The giant connected component of the remaining network structure serves as the relevant order parameter that shows the resilience of a macroscopic cluster in systems with information exchange such as epidemic spreading in social systems, financial transactions in stock markets, or transportation in urban networks, to mention a few examples. The simplest independent random removal rule leads to ordinary percolation [2,3], which shows a continuous phase transition for the emergence of a giant component. Various pruning strategies targeting centralities such as node degree [4–6] are often more deleterious in terms of disintegrating the network topology.

A paradigmatic pruning process deviating from the ordinary continuous phase transition is the k-core percolation [7,8]. The k core of a network is the maximal subgraph where each node has degree no less than k. It can be obtained by recursively removing nodes having fewer than k neighbors until no further deletion is possible. As a result, the network is decomposed into a collection of enclosed k cores, which has been extensively employed in the study of varied critical phenomena in the organization and dynamics of complex systems [9,10]. It is remarkable that the percolation threshold of a giant k-core cluster evinces a hybrid phase transition combining discontinuity and a critical singularity when $k \geqslant 3$ [1,7,8]. In contrast to the role of connected components in ordinary percolation, the k-core cluster is always giant in an infinite locally treelike network as finite k cores ($k \geqslant 2$) are absent therein. A deeper understanding of the network organization and robustness has been brought by some generalized models for k-core percolation, where spreading behavior [11], interdependence [12,13], and threshold heterogeneity [14] are factored in.

Recently, it has been considered that information accessible at a single node level in real complex systems is often nontopological, which is essential for quantifying the impact of percolation [15]. For example, the age and education level of individuals in contact networks are relevant for infectious disease outbreak [16]; body mass and feeding mode of species in food webs influences their resilience to adverse environmental perturbation [17,18]. This information, or metadata, characterizes the features of nodes that are distinct from conventional graph-theoretic centralities. A feature-enriched site percolation theory has been put forward in [15] by using degree-feature joint probability distributions. It is shown that the critical properties of networks under feature-based attacks are the same as those under mean-field percolation regardless of the feature distributions. However, the correlation between degree and feature has a nontrivial influence on the network robustness, allowing a more accurate evaluation of real network resilience.

It is worth noting that the nature of the feature is left undetermined in the general framework of feature-enriched percolation [15], whereas some specific forms of node feature have been examined in percolation models. For instance, healthiness of a node is considered in fractional percolation [19] and coreness of a node is incorporated as a feature under bond percolation in [20]. Moreover, the general idea of features or annotations has also been employed to aid network inference in supervised learning problems such as community

 ©2022 American Physical Society

detection in social networks [21,22] and link prediction in recommender systems [23,24].

Here we generalize the ordinary k-core percolation to the theory of feature-enriched core percolation taking into account both the generic node and edge features through a multiplex network approach. We introduce the concept of feature-enriched cores and describe a pruning process, finding them in a multiplex network with arbitrary degree distributions. Based on our theoretical framework, we determine some key quantities such as the corona cluster, relative size, and number of edges in the feature-enriched cores. A hybrid phase transition with a jump and a square root singularity is observed at the criticality of both the network connectivity and the node feature. We quantify the correlation between the degree and feature through the Farlie-Gumbel-Morgenstern distribution family and reveal an abrupt percolation transition at a critical correlation level for $k \geqslant 3$ in single networks. In the case of multiplex networks, we find that the feature-enriched core percolation is only continuous for the most outer cores and discontinuous for all inner cores in terms of connectivity and feature values. The evolution of the feature-enriched cores is limited by a characteristic curve of the feature distribution. Moreover, we find that asymmetric layer degree distributions can lead to crossovers in both network connectivity and feature space, which are nonexistent in identical layer distributions.

II. ANALYTICAL FRAMEWORK

Our method is based upon a unified representation of multiplex networks with m layers and n node features. The network is characterized by a joint degree-feature distribution $P(\boldsymbol{q}, \boldsymbol{\eta})$, where $\boldsymbol{q} = (q_1, q_2, \ldots, q_m) \in \mathbb{N}^m$ and $\boldsymbol{\eta} = (\eta_1, \eta_2, \ldots, \eta_n) \in \mathbb{R}^n$ represent the numbers of neighbors in all m layers and the n-dimensional feature space at each node, respectively. We construct the network ensemble by following the configuration model [25] with the degree sequence drawn from $P(\boldsymbol{q}) = \int P(\boldsymbol{q}, \boldsymbol{\eta}) d\boldsymbol{\eta}$ and assign features to each node following the conditional distribution $P(\boldsymbol{\eta}|\boldsymbol{q}) = P(\boldsymbol{q}, \boldsymbol{\eta})/P(\boldsymbol{q})$. Given $k = (k_1, k_2, \ldots, k_m)$ and $a = (a_1, a_2, \ldots, a_n)$, we define the $(\boldsymbol{k}, \boldsymbol{a})$ core of the multiplex network as its maximal subgraph having nodes with degree at least k_i in each layer i and feature value at least a_r for each $r = 1, 2, \ldots, n$. Here, for physical simplicity, we assume the features are continuous and regard them as some monotonic scores. Nevertheless, other variants such as discrete features or generic core criteria $\eta_r \in A_r$ for some set $A_r \subseteq \mathbb{R}$ are straightforward to produce in our framework.

As the network is locally treelike, we describe the following pruning process to uncover the $(\boldsymbol{k}, \boldsymbol{a})$ core. At every step we delete each node if it has degree $q_i < k_i$ in some layer i or it has feature value $\eta_r < a_r$ for some type r. If there are still such nodes left, we delete them in the next step. The process is repeated until no further deletion is possible. An illustration is shown in Fig. 1.

For each $i = 1, 2, \ldots, m$, let z_i be the probability that an end node of a randomly selected edge in layer i belongs to the $(\boldsymbol{k}, \boldsymbol{a})$ core, namely, it has feature value $\eta_r \geqslant a_r$ for $r = 1, 2, \ldots, n$ and has at least $k_i - 1$ neighbors in layer i and k_j neighbors in layer j for $j \neq i$ belonging to the $(\boldsymbol{k}, \boldsymbol{a})$ core. We

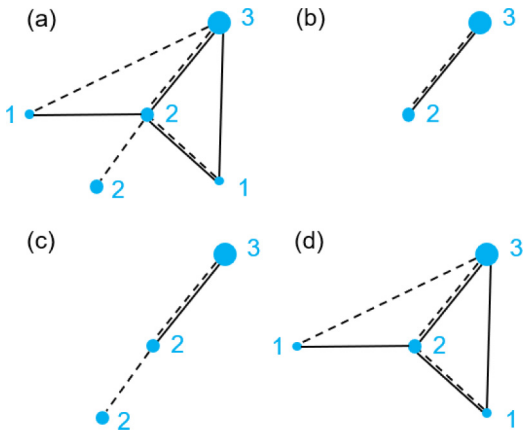

FIG. 1. Schematic of the $(\boldsymbol{k}, \boldsymbol{a})$ core for a network with $m = 2$ layers and $n = 1$ feature. (a) The network is shown with two different types of edges and blue numbers indicating values of the feature. (b) The $(\boldsymbol{k}, \boldsymbol{a})$ core for $\boldsymbol{k} = (1, 1)$ and $\boldsymbol{a} = 2$. Any increase of $\boldsymbol{k}$ or $\boldsymbol{a}$ would lead to the null core. (c) Core for $\boldsymbol{k} = (0, 0)$ and $\boldsymbol{a} = 2$, namely, a purely feature-based core. (d) Core for $\boldsymbol{k} = (1, 1)$ and $\boldsymbol{a} = 0$, which is a multiplex core irrespective of features.

write the self-consistent equation

$$z_i = \int_{\boldsymbol{a}}^{\infty} d\boldsymbol{\eta} \sum_{\boldsymbol{q}} \frac{q_i P(\boldsymbol{q}, \boldsymbol{\eta})}{\langle q_i \rangle} \times \left[\sum_{s=k_i-1}^{q_i-1} \binom{q_i - 1}{s} z_i^s (1 - z_i)^{q_i-1-s} \right] \times \prod_{\substack{j=1 \\ j \neq i}}^{m} \left[\sum_{s=k_j}^{q_j} \binom{q_j}{s} z_j^s (1 - z_j)^{q_j-s} \right], \tag{1}$$

where the integral $\int_{\boldsymbol{a}}^{\infty} d\boldsymbol{\eta}$ is interpreted as the multiple integral $\int_{a_1}^{\infty} \cdots \int_{a_n}^{\infty} d\eta_n \cdots d\eta_1$ and the sum of $\boldsymbol{q}$ is taken over all q_i from 0 to infinity. Here the average degree is calculated as $\langle q_i \rangle = \int_{-\infty}^{\infty} d\boldsymbol{\eta} \sum_{\boldsymbol{q}} q_i P(\boldsymbol{q}, \boldsymbol{\eta})$ and the excess degree-feature distribution $q_i P(\boldsymbol{q}, \boldsymbol{\eta})/\langle q_i \rangle$ represents the probability that the end node of a randomly selected edge in layer i has degree $\boldsymbol{q}$ and feature $\boldsymbol{\eta}$. The two combinatorial expressions in (1) indicate that no less than $k_i - 1$ out of $q_i - 1$ edges (excluding the starting edge) in layer i and no less than k_j out of q_j edges in layer j ($j \neq i$) lead to the $(\boldsymbol{k}, \boldsymbol{a})$ core.

The set of probabilities $\{z_i\}_{i=1}^m$ enable us to compute the probability $N_{(\boldsymbol{k},\boldsymbol{a})}$ that a random node is in the $(\boldsymbol{k}, \boldsymbol{a})$ core, which is the relative size of the feature-enriched core in the network. A node is in the $(\boldsymbol{k}, \boldsymbol{a})$ core if it has feature value $\eta_r \geqslant a_r$ for $r = 1, 2, \ldots, n$ and no less than k_i edges in layer i leading to the $(\boldsymbol{k}, \boldsymbol{a})$ core for $i = 1, 2, \ldots, m$. Therefore, we obtain

$$N_{(\boldsymbol{k},\boldsymbol{a})} = \int_{\boldsymbol{a}}^{\infty} d\boldsymbol{\eta} \sum_{\boldsymbol{q}} P(\boldsymbol{q}, \boldsymbol{\eta}) \times \prod_{i=1}^{m} \left[\sum_{s=k_i}^{q_i} \binom{q_i}{s} z_i^s (1 - z_i)^{q_i-s} \right]. \tag{2}$$

To analytically solve (1) and (2), we can introduce conditional generating functions by assuming that the multiplex network has uncorrelated degrees between layers, namely, $P(\boldsymbol{q},\boldsymbol{\eta}) = P(\boldsymbol{\eta})\cdot\prod_{i=1}^{m} P(q_i|\boldsymbol{\eta})$ for $\boldsymbol{q}\in\mathbb{N}^m$ and $\boldsymbol{\eta}\in\mathbb{R}^n$, where $P(\boldsymbol{\eta}) = \sum_{\boldsymbol{q}} P(\boldsymbol{q},\boldsymbol{\eta})$ and $P(q_i|\boldsymbol{\eta}) = P(q_i,\boldsymbol{\eta})/P(\boldsymbol{\eta})$ for $i = 1,2,\ldots,m$. For each given i, define the generating function

$$G_i(x|\boldsymbol{\eta}) = \sum_{q_i=0}^{\infty} P(q_i|\boldsymbol{\eta})x^{q_i}. \tag{3}$$

The sth derivative of G_i is defined by $G_i^{(s)}(x|\boldsymbol{\eta}) = \sum_{q_i\geqslant s} P(q_i|\boldsymbol{\eta})\frac{q_i!}{(q_i-s)!}x^{q_i-s}$. By some calculations, Eqs. (1) and (2) can be recast as

$$z_i = \int_{\boldsymbol{a}}^{\infty} d\boldsymbol{\eta}\, P(\boldsymbol{\eta})\left(1-\frac{1}{\langle q_i\rangle}\sum_{s=0}^{k_i-2}\frac{G_i^{(s+1)}(1-z_i|\boldsymbol{\eta})}{s!}z_i^s\right)\times\prod_{\substack{j=1\\ j\neq i}}^{m}\left(1-\sum_{s=0}^{k_j-1}\frac{G_j^{(s)}(1-z_j|\boldsymbol{\eta})}{s!}z_j^s\right) \tag{4}$$

and

$$N_{(\boldsymbol{k},\boldsymbol{a})} = \int_{\boldsymbol{a}}^{\infty} d\boldsymbol{\eta}\, P(\boldsymbol{\eta})\times\prod_{i=1}^{m}\left(1-\sum_{s=0}^{k_i-1}\frac{G_i^{(s)}(1-z_i|\boldsymbol{\eta})}{s!}z_i^s\right). \tag{5}$$

Based on these equations, we can determine the singularity for the order parameters $\{z_i\}_{i=1}^m$ at criticality. In feature-enriched core percolation, there are naturally two sets of control parameters: One regulates the topology and the other the features. In Appendix A we show that in both cases, the critical exponents are $1/2$, namely, take the same value for the ordinary core percolation.

Moreover, let $N_{(\boldsymbol{k},\boldsymbol{a})}(\boldsymbol{q},\boldsymbol{\eta})$ be the fraction of nodes with degrees $\boldsymbol{q}$ and feature values $\boldsymbol{\eta}$ that are in the $(\boldsymbol{k},\boldsymbol{a})$ core. Here the feature values are interpreted as in the infinitesimal hypercube $[\boldsymbol{\eta},\boldsymbol{\eta}+\mathrm{d}\boldsymbol{\eta}]$ by convention since features are continuous. Clearly, if $q_i < k_i$ for some i or $\eta_r < a_r$ for some r, then $N_{(\boldsymbol{k},\boldsymbol{a})}(\boldsymbol{q},\boldsymbol{\eta}) = 0$. Otherwise, we have

$$N_{(\boldsymbol{k},\boldsymbol{a})}(\boldsymbol{q},\boldsymbol{\eta}) = \sum_{\boldsymbol{s}\geqslant\boldsymbol{q}} P(\boldsymbol{s},\boldsymbol{\eta})\times\prod_{i=1}^{m}\left[\binom{s_i}{q_i}z_i^{q_i}(1-z_i)^{s_i-q_i}\right], \tag{6}$$

where $\boldsymbol{s} = (s_1,s_2,\ldots,s_m)$ and the sum $\sum_{\boldsymbol{s}\geqslant\boldsymbol{q}}$ is taken over $s_i\geqslant q_i$ for all i. In k-core decomposition, an important concept is the corona cluster [8], which is the subgraph of nodes with degree k in the k core. We can extend this concept to feature-enriched corona as the subgraph containing nodes with degree $\boldsymbol{k}$ and feature value at least $\boldsymbol{a}$ (dimensionwise). Assuming the conditional independence of the degrees as before, we can derive its relative size as

$$N_{(\boldsymbol{k},\boldsymbol{a})}(\boldsymbol{k}) := \int_{\boldsymbol{a}}^{\infty} d\boldsymbol{\eta}\, N_{(\boldsymbol{k},\boldsymbol{a})}(\boldsymbol{k},\boldsymbol{\eta}) = \int_{\boldsymbol{a}}^{\infty} d\boldsymbol{\eta}\, P(\boldsymbol{\eta})\times\prod_{i=1}^{m}\left(\frac{G_i^{(k_i)}(1-z_i|\boldsymbol{a})}{k_i!}z_i^{k_i}\right), \tag{7}$$

where we have applied (6) and the generating function (3). If the feature $\boldsymbol{\eta}$ is discrete, we can alternatively define the feature-enriched corona as the subgraph containing nodes with degree $\boldsymbol{k}$ and feature value $\boldsymbol{a}$. Hence, in analogy to (7), this alternative version of corona follows

$$N_{(\boldsymbol{k},\boldsymbol{a})}(\boldsymbol{k},\boldsymbol{a}) = P(\boldsymbol{a})\prod_{i=1}^{m}\left(\frac{G_i^{(k_i)}(1-z_i|\boldsymbol{a})}{k_i!}z_i^{k_i}\right). \tag{8}$$

Define $L_{(\boldsymbol{k},\boldsymbol{a})}$ as the relative number of edges in the $(\boldsymbol{k},\boldsymbol{a})$ core normalized by the size of the core. As each edge contributes two degrees, it is easy to see that the following equation holds:

$$L_{(\boldsymbol{k},\boldsymbol{a})} = \frac{1}{2}\int_{\boldsymbol{a}}^{\infty} d\boldsymbol{\eta}\times\sum_{\boldsymbol{q}}(q_1+q_2+\cdots+q_m)N_{(\boldsymbol{k},\boldsymbol{a})}(\boldsymbol{q},\boldsymbol{\eta}). \tag{9}$$

Assuming the conditional independence of the degrees and using (6), we can rewrite (9) as

$$L_{(\boldsymbol{k},\boldsymbol{a})} = \frac{1}{2}\int_{\boldsymbol{a}}^{\infty} d\boldsymbol{\eta}\, P(\boldsymbol{\eta})\times\sum_{\boldsymbol{q}}\sum_{j=1}^{m} q_j\prod_{i=1}^{m}\left(\frac{G_i^{(q_i)}(1-z_i|\boldsymbol{\eta})}{q_i!}z_i^{q_i}\right). \tag{10}$$

III. RESULTS FOR SINGLE NETWORKS

As a representative example, we here consider Erdős-Rényi (ER) networks (Poisson degree distributions) with a single layer, i.e., $m = 1$. The marginal degree distribution is $P(q) = e^{-\lambda}\lambda^q/q!$ for $q\geqslant 0$, where the parameter $\lambda = \langle q\rangle$ is the average degree. We assume the feature space is one dimensional and follows the standard normal distribution, namely, $n = 1$ and the feature admits the marginal probability density $P(\eta) = \varphi(\eta) := (2\pi)^{-1/2}e^{-\eta^2/2}$ for $\eta\in\mathbb{R}$ and the marginal distribution function is given by $\Phi(\eta) = \int_{-\infty}^{\eta}\varphi(y)dy$.

A. Uncorrelated degree and feature

In the uncorrelated case, the joint degree-feature distribution of the network becomes $P(q,\eta) = (2\pi)^{-1/2}e^{-\lambda-\eta^2/2}\lambda^q/q!$. This allows us to analytically reveal the interplay between topology and feature in core structures. For example, we find $L_{(k,a)}\sim\frac{\lambda}{2}[1-\Phi(a)]N_{(k,a)}$ for $a\in\mathbb{R}$ when k is large (see Appendix B). Figure 2 shows the behavior of feature-enriched core percolation for small k with respect to different λ and a. The agreement between simulations and theory is very good. Some remarks are as follows.

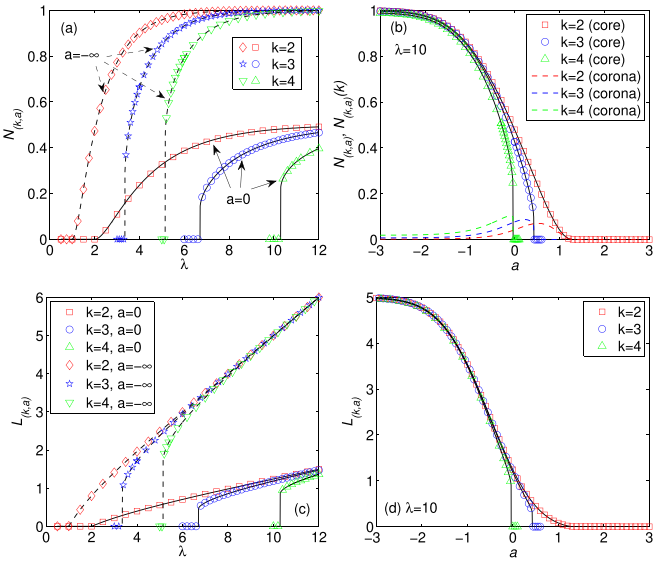

FIG. 2. (a) and (b) Relative size of the (k, a) core for ER networks of size $N = 10^6$ with average degree λ for different $k = 2$ (red plots), $k = 3$ (blue plots), $k = 4$ (green plots), and feature value a. The corona cluster size is also shown in (b). (c) and (d) Relative edge numbers of the (k, a) core for the corresponding ER networks. Solid and dashed lines are based on theory and symbols are simulations averaged over 100 network realizations.

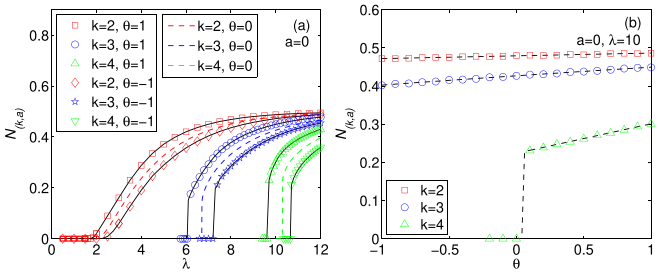

FIG. 3. (a) Relative size of the $(k, 0)$ core for ER networks of size $N = 10^6$ with average degree λ for different $k = 2$ (red plots), $k = 3$ (blue plots), $k = 4$ (green plots), and θ. (b) Relative size of the $(k, 0)$ core as a function of θ for ER networks with $\lambda = 10$. Solid and dashed lines are based on theory and symbols are simulations averaged over 100 network realizations.

First, we observe that the size $N_{(k,a)}$ of the (k, a) core experiences a continuous phase transition in terms of not only the network connectivity [Fig. 2(a)] but the feature value [Fig. 2(b)] when $k = 2$. When $k \geqslant 3$, the percolation behaviors become discontinuous at the critical points. When the node feature is taken into account, the simple order of enclosed k cores is broken, giving a landscape of feature-enriched cores. For instance, for an ER network with $\lambda = 4$, its 3 core [or equivalently its $(3, -\infty)$ core] nearly triples its (2,0) core [cf. Fig. 2(a)]. There is also a region around $\lambda = 6$ where the (3,0) core vanishes but the 4 core remains quite strong.

Second, the nonmonotonicity of the corona cluster shown in Fig. 2(b) is qualitatively similar to the phenomenon in ordinary core percolation under attacks [8]. This is because the parameter a here plays a similar role of occupation probability in the uncorrelated situation. However, noting that the feature assumes the standard normal distribution, we observe that the humps of the corona curves are around the mean value $a = 0$ of the feature distribution and dying away beyond, for example, the 3-σ range (which is always the case at least for small k), in line with the statistical characteristics of a normal distribution. This feature distribution relevant phenomenon may be helpful in determining cortical regions of degeneration in brain networks [26,27] and is fundamentally different from the ordinary corona evolution under attacks.

On top of the size of the (k, a) core, the relative number $L_{(k,a)}$ of edges shows analogous structural transitions at the same critical points in terms of network connectivity [Fig. 2(c)] and feature values [Fig. 2(d)]. By the definition in (9), it is easy to check that $2L_{(\boldsymbol{k},\boldsymbol{a})}$ is the average degree or density of the $(\boldsymbol{k}, \boldsymbol{a})$ core. Comparing Figs. 2(a) and 2(c), we observe that as a grows from $-\infty$ to 0, the size of the (k, a) core is shrunk roughly by half but its density is reduced by about three-quarters. The qualitative relation can also be verified by the expressions (B2) and (B3). This phenomenon indicates that, compared to the size, the density of a core is more sensitive to the variation of features.

B. Correlated degree and feature

Next we study single networks with correlated degree and feature distributions by employing the bivariate Farlie-Gumbel-Morgenstern (FGM) copula [28]. We consider the joint cumulative degree-feature distribution

$$F(q, \eta) = F_1(q)F_2(\eta) \times \{1 + \theta[1 - F_1(q)][1 - F_2(\eta)]\}, \quad (11)$$

where $F_1(q) = e^{-\lambda} \sum_{s=0}^{q} \lambda^s/s!$ is the cumulative degree distribution for ER networks and $F_2(\eta)$ is chosen as the cumulative feature distribution for a uniform random variable over $\{-1, 1\}$. It is not difficult to see that (11) gives the right distribution since $F_1(\infty) = F_2(\infty) = 1$, $F(q, \infty) = F_1(q)$, and $F(\infty, \eta) = F_2(\eta)$. Here $|\theta| \leqslant 1$ is the parameter controlling the coupling strength of the two marginal distributions. The degree and feature are positively correlated if $\theta > 0$ and they are negatively correlated if $\theta < 0$. When $\theta = 0$, the degree and feature become independent.

Note that we here consider a discrete feature to avoid the mixed joint distribution. Since $F_2(0) = \Phi(0) = 1/2$, the $(k, 0)$ core is equivalent to the corresponding scenario explored in Sec. III A when $\theta = 0$ due to the symmetry of the feature distributions. In Fig. 3 we show the behavior of $(k, 0)$ core for different λ and θ.

It is immediate to observe that the positive correlation enhances the feature-enriched cores whereas the negative correlation diminishes them. This phenomenon holds for all k. It can be explained as follows. When nodes of degree less than k are removed, they tend to be those with low features (which will be deleted anyway under the feature-based rule) if there is a positive correlation. Therefore, fewer nodes are removed overall, which gives rise to a stronger core. Likewise, in the case of negative correlation, those nodes having low

degrees tend to have higher features, leading to more deletion in the feature-enriched pruning process. Remarkably, the correlation does not alter the nature of the phase transition for core percolation, namely, $k = 3$ remains the separatrix for the continuous and discrete percolation transition.

The change of the $(k, 0)$ core with respect to θ shown in Fig. 3(b) indicates the existence of an abrupt percolation transition for $k \geqslant 3$ (the figure shows the case for $k = 4$). This underscores the nontriviality of the role of correlation between the degree and feature. As suggested in [15], features can be related to network construction and dynamical processes on top of the network in reality, which naturally lead to some sort of correlation. It is also worth mentioning that the FGM family is limited to characterize weak correlation only, with the correlation coefficient in $[-1/3, 1/3]$ [28]. This explains the gentle increments relevant to θ in Fig. 3(b).

IV. RESULTS FOR DUPLEX NETWORKS

To appreciate both the node and edge features incorporated in our theoretical framework, in this section we consider networks with two layers, namely, $m = 2$. For the sake of simplicity, we restrict ourselves to the case of uncorrelated degrees and features. We first consider the symmetric situation in Secs. IV A and IV B, where both layers have the same distributions, and then examine an asymmetric situation in Sec. IV C for completion. We take $n = 1$ and the node feature is chosen again as the standard normal distribution with probability density $\varphi(\eta) = (2\pi)^{-1/2} e^{-\eta^2/2}$ for $\eta \in \mathbb{R}$. For a general number m of layers, we can show that for any given $\boldsymbol{k} = (k_1, k_2, \ldots, k_m) \in \mathbb{N}^m$ and $a \in \mathbb{R}$, $N_{(\boldsymbol{k},a)} \sim [1 - \Phi(a)][1 - \rho(\boldsymbol{k})]^m$ for some $\rho(\boldsymbol{k}) \in [0, 1]$ relying on the network topology (see Appendix C for general results).

A. Networks with Poisson degree distributions

Assume that the two layers in the network have the Poisson degree distributions $P(q_1) = e^{-\lambda_1} \lambda_1^{q_1}/q_1!$ and $P(q_2) = e^{-\lambda_2} \lambda_2^{q_2}/q_2!$ with $\lambda =: \lambda_1 = \lambda_2$. In Figs. 4(a) and 4(b) we show the behavior of $N_{(\boldsymbol{k},a)}$ for the duplex ER network scenario with $\boldsymbol{k} = (k_1, k_2)$.

The feature-enriched $(\boldsymbol{k}, a)$ core displays a continuous percolation transition in the case of $\boldsymbol{k} = (1, 1)$. However, there is a jump at the critical point of the network connectivity when $k_1 + k_2 \geqslant 3$ [cf. Fig. 4(a)]. This phenomenon is qualitatively consistent with some other models of core percolation under multiplex topologies [12,29]. As in the case of single networks, the continuous or discontinuous phase transition nature for topology maps to the feature space in the multiplex network setting. Figure 4(b) shows that the continuous transition exists only for the $(\boldsymbol{k}, a)$ core with $\boldsymbol{k} = (1, 1)$. For any $\boldsymbol{k}$ and a, the relative size of the $(\boldsymbol{k}, a)$ core is under the characteristic curve $1 - \Phi(a)$ of the feature, which agrees with our theory. Note that the gap between them is minimal for a significant proportion of a [e.g., $a \in (-\infty, 0)$] even for inner cores, highlighting the robustness of ER-ER topology. Furthermore, in the spirit of robustness measure R [30], it seems plausible to quantify network robustness against feature-based attacks

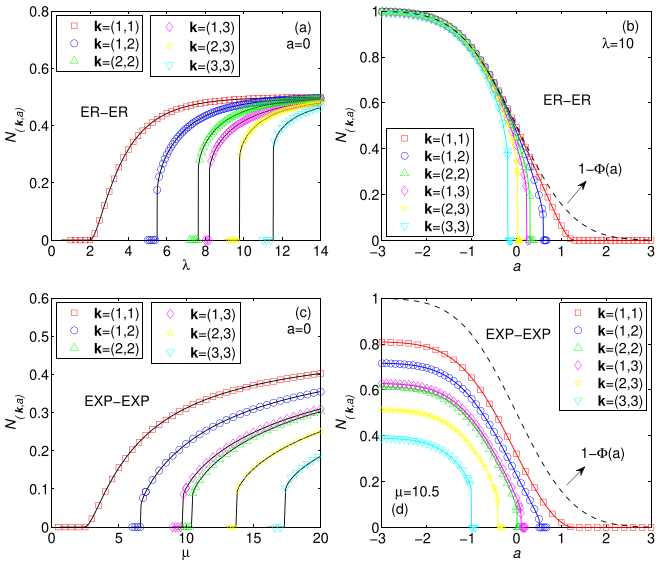

FIG. 4. (a) and (b) Relative size of the $(\boldsymbol{k}, a)$ core for duplex ER networks of size $N = 10^6$ with average degree λ for different $\boldsymbol{k} = (1, 1)$ (red plots), $\boldsymbol{k} = (1, 2)$ (blue plots), $\boldsymbol{k} = (2, 2)$ (green plots), $\boldsymbol{k} = (1, 3)$ (magenta plots), $\boldsymbol{k} = (2, 3)$ (yellow plots), $\boldsymbol{k} = (3, 3)$ (cyan plots), and feature value a. (c) and (d) Relative size of the $(\boldsymbol{k}, a)$ core for duplex EXP networks of size $N = 10^6$ with the parameter μ for different degree $\boldsymbol{k}$ and feature a analogously. Solid and dashed lines are based on theory and symbols are simulations averaged over 100 network realizations.

by calculating the area between the two curves $N_{(\boldsymbol{k},a)}$ and $1 - \Phi(a)$ over the whole range of a.

B. Networks with exponential degree distributions

Next we consider the duplex networks with two identical exponential (EXP) degree distributions, namely, $P(q) = (1 - e^{-1/\mu}) e^{-q/\mu}$ for $q \geqslant 0$. Such networks have a heterogeneous degree distribution with the parameter $\mu = 1/\ln(1 + 1/\langle q \rangle) \sim \langle q \rangle$ approximating the mean degree of (a layer of) the network [25]. The corresponding results of $N_{(\boldsymbol{k},a)}$ in this type of network are shown in Figs. 4(c) and 4(d).

As one would expect, the hybrid phase transitions also exist in the duplex EXP networks. However, the duplex EXP networks have smaller feature-enriched cores than the corresponding duplex ER networks with the same mean degree or density. This holds true across the range of all feature values. Note that $\mu = 10.5$ set in Fig. 4(d) is equivalent to an average degree $\langle q \rangle \approx 10$.

Comparing Figs. 4(a) and 4(b) with Figs. 4(c) and 4(d), we interestingly observe that $N_{((2,2),a)}(\text{ER-ER}) \geqslant N_{((1,3),a)}(\text{ER-ER})$ whereas $N_{((2,2),a)}(\text{EXP-EXP}) \leqslant N_{((1,3),a)}(\text{EXP-EXP})$ for all a. The relationship among $N_{((k_1,k_2),a)}$ when $k_1 + k_2 \equiv$ const certainly relies on the specific network topology, but an insight here is that an uncorrelated feature would not change the size order among them. This is potentially applicable as the core decomposition sequence in multiplex networks is found to be correlated with geometric embedding of real networks [31] as well as certain functional areas revealed by brain-computer interface training [32].

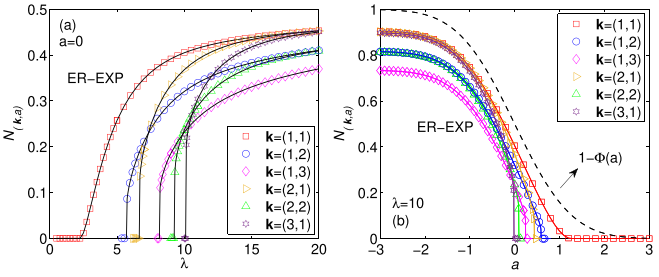

FIG. 5. Relative size of the $(\boldsymbol{k}, a)$ core for ER-EXP networks of size $N = 10^6$ with average degree $\lambda = \mu$ for different $\boldsymbol{k} = (1, 1)$ (red plots), $\boldsymbol{k} = (1, 2)$ (blue plots), $\boldsymbol{k} = (2, 2)$ (green plots), $\boldsymbol{k} = (1, 3)$ (magenta plots), $\boldsymbol{k} = (2, 1)$ (khaki plots), $\boldsymbol{k} = (3, 1)$ (purple plots), and feature value a. Solid and dashed lines are based on theory and symbols are simulations averaged over 100 network realizations.

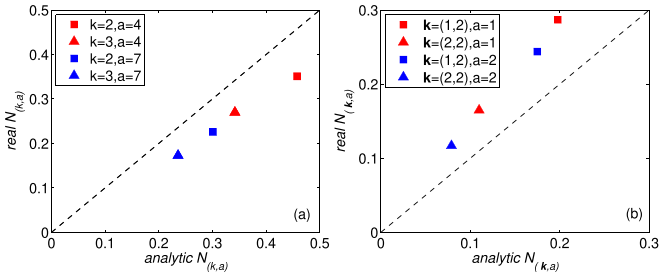

FIG. 6. (a) Relative size of the (k, a) core for SEM and its randomized version with $k = 2$ and $a = 4$ (red square), $k = 3$ and $a = 4$ (red triangle), $k = 2$ and $a = 7$ (blue square), and $k = 3$ and $a = 7$ (blue triangle). (b) Relative size of the $(\boldsymbol{k}, a)$ core for FIN and its randomized version with $k = (1, 2)$ and $a = 1$ (red square), $k = (2, 2)$ and $a = 1$ (red triangle), $k = (1, 2)$ and $a = 2$ (blue square), and $k = (2, 2)$ and $a = 2$ (blue triangle).

C. Networks with asymmetric layer degree distributions

Finally, we examine an asymmetric duplex network ER-EXP, namely, one layer follows the Poisson degree distribution $P(q) = e^{-\lambda}\lambda^q/q!$ and the other layer follows the exponential degree distribution $P(q) = (1 - e^{-1/\mu})e^{-q/\mu}$, with $\mu = \lambda$ and $q \geqslant 0$. The results of $N_{(\boldsymbol{k},a)}$ are shown in Figs. 5(a) and 5(b).

The hybrid phase transition of the feature-enriched $(\boldsymbol{k}, a)$ core regarding the different combinations of k_1 and k_2 remains consistent with the above symmetric scenarios. However, we observe several remarkable crossover phenomena in the network topological space. For example, the crossovers among $N_{((2,2),a)}$(ER-EXP), $N_{((1,3),a)}$(ER-EXP), and $N_{((3,1),a)}$(ER-EXP) in Fig. 5(a) indicate that within a certain range of λ, one of these feature-enriched cores can be more robust than the other two. This is in sharp contrast to the symmetric cases in Figs. 4(a) and 4(c). Moreover, in the feature space, we also observe similar crossover phenomena in Fig. 5(b) at a given λ, which are nonexistent in Figs. 4(b) and 4(d). This suggests a deeper nexus between the node feature and network topology and again highlights the nontriviality of the feature-enriched core percolation even in the simplest scenario of uncorrelated degrees and features.

V. REAL NETWORK EXAMPLES

In this section we consider two real-world networks to show the effectiveness of our feature-enriched percolation framework. The first network SEM is a semantic association network of the Edinburgh Associative Thesaurus [33] with 23 219 nodes and 325 029 edges. This is a single network, in which nodes are phrases and two nodes are connected by an edge if they are associated in the word association user experiments. The node feature is taken as the length of the phrase ranging from 0 to 28. The second network FIN is a financial market network of China [34], where nodes are companies and two nodes are joined if they have a liability guarantee relationship. This network contains 4354 nodes and is duplex with the first layer (for the year 2013) having 3618 edges and the second layer (for the year 2014) having 4102 edges. We take the node feature as the current ratio at December, which ranges from 0.13 to 10.74.

We show in Fig. 6 the feature-enriched core size $N_{(\boldsymbol{k},a)}$ in these two networks for different $\boldsymbol{k}$ and a against that the analytic results in the randomized versions. To generate the joint degree-feature distributions of the corresponding randomized networks, we assume the degree distributions in the two layers in the FIN network are independent. Note that the higher-dimensional copula takes the same format of (11) since the only correlation we consider here is between the degree and feature [35]. The empirical degree distributions and the degree-feature correlation parameters $\theta_{\text{SEM}} = -0.31$ and $\theta_{\text{FIN}} = 0.47$ are then fed into the corresponding FGM copulas to calculate the theoretical results. We observe from Fig. 6 that there are some differences in the feature-enriched core sizes between real networks and analytic results. This is arguably due to the presence of intricate structures such as interlayer degree correlation, assortativity, clustering, and communities, which all influence the percolation process.

VI. CONCLUSION

The theory of k-core percolation is an important tool for understanding network structure and resilience. In this paper we have introduced the concept of the feature-enriched $(\boldsymbol{k}, \boldsymbol{a})$ core and presented a general framework for $(\boldsymbol{k}, \boldsymbol{a})$-core percolation over multiplex networks. We have analytically derived the corona cluster, size, and number of edges of the $(\boldsymbol{k}, \boldsymbol{a})$ core. A hybrid phase transition combining a jump and a square root singularity was observed at the critical points in both the network topology and the feature space. The influence of correlation between degree and feature was demonstrated through the FGM family, which favorably characterizes a continuous variation of correlation between two distributions with given marginals. We found that the (k, a) core grows monotonically with the correlation and that a first-order percolation transition occurs at a critical correlation level for $k \geqslant 3$ in single networks. In the duplex network scenarios, we show that the transitions for the $(\boldsymbol{k}, a)$ core are continuous only for $\boldsymbol{k} = (1, 1)$ and more inner cores display an abrupt percolation transition in terms of the connectivity as well as the feature, limited by a characteristic curve when the feature space is one dimensional. We hope this work can be a helpful starting point for the development of new feature-enriched

percolation models and analytical and phenomenological studies in feature-rich complex systems.

APPENDIX A: CRITICAL EXPONENTS OF THE PHASE TRANSITION

The set of equations in (4) can be represented by $z_i = f_i(z_1, z_2, \ldots, z_m)$ for $i = 1, 2, \ldots, m$. Let $\lambda_i := \langle q_i \rangle$ be the control parameter for the network topology. At $N_{(\boldsymbol{k},\boldsymbol{a})} = 0$ we have the critical points $\{z_{ic}\}_{i=1}^m$, where the $(\boldsymbol{k}, \boldsymbol{a})$ core starts to emerge. From (5) we observe no special behavior at $\{z_{ic}\}_{i=1}^m$ and that the singularity of $N_{(\boldsymbol{k},\boldsymbol{a})}$ comes from $\{\lambda_i\}_{i=1}^m$ in (4). When $\{\lambda_i\}_{i=1}^m$ are small, the system only has trivial solutions $z_i = 0$ for $i = 1, 2, \ldots, m$ and hence there is no $(\boldsymbol{k}, \boldsymbol{a})$ core. The critical points are the largest nontrivial solutions $z_i \in (0, 1]$, which can be obtained by solving the system (4) along with the determinant $|I - J| = 0$ invoking the implicit function theorem, where $I \in \mathbb{R}^{m\times m}$ is the identity matrix and $J = (\frac{\partial f_i}{\partial z_j}) \in \mathbb{R}^{m\times m}$ is the Jacobian matrix.

For simplicity, we consider a symmetric scenario, where all layers have the same degree distribution, $\boldsymbol{k} = (k, k, \ldots, k) \in \mathbb{R}^m$, and $\boldsymbol{a} = a \in \mathbb{R}$. Hence, we have $\lambda_i \equiv \lambda$ for $i = 1, 2, \ldots, m$ and write (4) as $z = f(z, \lambda)$, where z is the single order parameter. (Note that f is also a function of features, but they are taken as constants for now for the sake of clarity.) We set $z = z_c + \varepsilon$ and $\lambda = \lambda_c + \delta$ and perform the Taylor expansion at $\varepsilon \to 0$ and $\delta \to 0$:

$$z_c + \varepsilon = f(z_c, \lambda_c) + \frac{\partial}{\partial z} f(z_c, \lambda_c)\varepsilon + + \frac{\partial}{\partial \lambda} f(z_c, \lambda_c)\delta + \frac{1}{2!}\frac{\partial^2}{\partial z^2} f(z_c, \lambda_c)\varepsilon^2 + o(\delta) + o(\varepsilon^2). \tag{A1}$$

Noting that $z_c = f(z_c, \lambda_c)$ and $1 = \frac{\partial}{\partial z} f(z_c, \lambda_c)$, we have from (A1) that

$$\varepsilon = z - z_c \propto (\lambda - \lambda_c)^{1/2}. \tag{A2}$$

For the feature space, we may take, for example, the expectation $\mu := \int \eta P(\eta) d\eta$ as the control parameter. Then Eq. (4) is written as $z = f(z, \mu)$. By setting $z = z_c + \varepsilon$ and $\mu = \mu_c + \zeta$ and performing the expansion at $\varepsilon \to 0$ and $\zeta \to 0$, we obtain similarly

$$\varepsilon = z - z_c \propto (\mu - \mu_c)^{1/2}. \tag{A3}$$

The enriched-core percolation is a hybrid phase transition with a jump of the order parameters and a square root singularity at the criticality. The general cases can be shown with a similar procedure but more tedious calculations because vector-valued functions are used for the expansion.

APPENDIX B: UNCORRELATED DEGREE AND FEATURE IN SINGLE NETWORKS

In uncorrelated networks with a Poisson degree distribution $P(q) = e^{-\lambda}\lambda^q/q!$ and a standard normal feature η, we can derive

$$z = [1 - \Phi(a)]\left(1 - e^{-\lambda z}\sum_{s=0}^{k-2}\frac{(\lambda z)^s}{s!}\right) \tag{B1}$$

and

$$N_{(k,a)} = [1 - \Phi(a)]\left(1 - e^{-\lambda z}\sum_{s=0}^{k-1}\frac{(\lambda z)^s}{s!}\right) \tag{B2}$$

by employing (4), (5), and the generating function $G(x) = e^{\lambda(x-1)}$. Using (B1) and (10), we have

$$L_{(k,a)} = [1 - \Phi(a)]\frac{\lambda z}{2} = \frac{\lambda}{2}[1 - \Phi(a)]^2\left(1 - e^{-\lambda z}\sum_{s=0}^{k-2}\frac{(\lambda z)^s}{s!}\right). \tag{B3}$$

In view of (B2) and (B3), we obtain

$$L_{(k,a)} \sim \frac{\lambda}{2}[1 - \Phi(a)]N_{(k,a)} \tag{B4}$$

for large k, by applying the Stirling formula.

APPENDIX C: CORE SIZE IN MULTIPLEX NETWORKS

For the ease of presentation, we begin with a multiplex network with m layers following the same Poisson degree distribution $P(q) = e^{-\lambda}\lambda^q/q!$ and an uncorrelated feature η following the standard normal distribution. If $\boldsymbol{k} = (k, k, \ldots, k) \in \mathbb{N}^m$, we obtain by (4) and (5) that

$$z = [1 - \Phi(a)]\left(1 - e^{-\lambda z}\sum_{s=0}^{k-2}\frac{(\lambda z)^s}{s!}\right) \times \left(1 - e^{-\lambda z}\sum_{s=0}^{k-1}\frac{(\lambda z)^s}{s!}\right)^{m-1} \tag{C1}$$

and

$$N_{(\boldsymbol{k},a)} = [1 - \Phi(a)]\left(1 - e^{-\lambda z}\sum_{s=0}^{k-1}\frac{(\lambda z)^s}{s!}\right)^m. \tag{C2}$$

When λ is small, Eq. (C1) only has a trivial solution $z = 0$ and hence $N_{(\boldsymbol{k},a)} \equiv 0$ by (C2). When λ is sufficiently large, Eq. (C1) begins to have positive solutions and $N_{(\boldsymbol{k},a)} = [1 - \Phi(a)][1 - \rho(k)]^m$, where $\rho(k) \in (0, 1)$ depending on the degree distribution. Hence, $N_{(\boldsymbol{k},a)} \leqslant 1 - \Phi(a)$, where the upper bound is not achievable in ER networks.

For general (but layer-identical) degree and (potentially correlated) feature distributions, the same argument gives us $N_{(\boldsymbol{k},\boldsymbol{a})} = [1 - \rho(k)]^m \int_{\boldsymbol{a}}^{\infty} d\boldsymbol{\eta} P(\boldsymbol{\eta})$ for some $\rho(k) \in [0, 1]$ depending on the degree distribution and correlation. When the network has different layer degree distributions and general $\boldsymbol{k} = (k_1, k_2, \ldots, k_m)$, we can similarly obtain $N_{(\boldsymbol{k},\boldsymbol{a})} \sim [1 - \rho(\boldsymbol{k})]^m \int_{\boldsymbol{a}}^{\infty} d\boldsymbol{\eta} P(\boldsymbol{\eta})$, where $\rho(\boldsymbol{k}) \in [0, 1]$ relying on the degrees and their correlation with features.

[1] M. Li, R.-R. Liu, L. Lü, M.-B. Hu, S. Xu, and Y.-C. Zhang, Phys. Rep. **907**, 1 (2021).

[2] D. S. Callaway, M. E. J. Newman, S. H. Strogatz, and D. J. Watts, Phys. Rev. Lett. **85**, 5468 (2000).

[3] R. Cohen and S. Havlin, *Percolation in Complex Networks* (Springer, New York, 2021), pp. 419–431.

[4] R. Albert, H. Jeong, and A.-L. Barabási, Nature (London) **406**, 378 (2000).

[5] S. Iyer, T. Killingback, B. Sundaram, and Z. Wang, PLoS ONE **8**, e59613 (2013).

[6] Y. Shang, Phys. Rev. E **103**, 042316 (2021).

[7] S. N. Dorogovtsev, A. V. Goltsev, and J. F. F. Mendes, Phys. Rev. Lett. **96**, 040601 (2006).

[8] A. V. Goltsev, S. N. Dorogovtsev, and J. F. F. Mendes, Phys. Rev. E **73**, 056101 (2006).

[9] Y.-X. Kong, G.-Y. Shi, R.-J. Wu, and Y.-C. Zhang, Phys. Rep. **832**, 1 (2019).

[10] F. D. Malliaros, C. Giatsidis, A. N. Papadopoulos, and M. Vazirgiannis, VLDB J. **29**, 61 (2020).

[11] Y. Shang, SIAM J. Appl. Math. **80**, 1272 (2020).

[12] N. Azimi-Tafreshi, J. Gómez-Gardeñes, and S. N. Dorogovtsev, Phys. Rev. E **90**, 032816 (2014).

[13] N. K. Panduranga, J. Gao, X. Yuan, H. E. Stanley, and S. Havlin, Phys. Rev. E **96**, 032317 (2017).

[14] D. Cellai, A. Lawlor, K. A. Dawson, and J. P. Gleeson, Phys. Rev. Lett. **107**, 175703 (2011).

[15] O. Artime and M. D. Domenico, Nat. Commun. **12**, 2478 (2021).

[16] N. Perra, Phys. Rep. **913**, 1 (2021).

[17] U. Brose *et al.*, Nat. Ecol. Evol. **3**, 919 (2019).

[18] L. Pecuchet, M.-A. Blanchet, A. Frainer, B. Husson, L. L. Jørgensen, S. Kortsch, and R. Primicerio, Global Change Biol. **26**, 4894 (2020).

[19] Y. Shang, Phys. Rev. E **89**, 012813 (2014).

[20] A. Allard and L. Hébert-Dufresne, Phys. Rev. X **9**, 011023 (2019).

[21] D. Hric, T. P. Peixoto, and S. Fortunato, Phys. Rev. X **6**, 031038 (2016).

[22] L. Peel, D. B. Larremore, and A. Clauset, Sci. Adv. **3**, e1602548 (2017).

[23] M. E. J. Newman and A. Clauset, Nat. Commun. **7**, 11863 (2016).

[24] O. Fajardo-Fontiveros, R. Guimerá, and M. Sales-Pardo, Phys. Rev. X **12**, 011010 (2022).

[25] M. E. J. Newman, *Networks*, 2nd ed. (Oxford University Press, Oxford, 2018).

[26] F. Battiston, J. Guillon, M. Chavez, V. Latora, and F. D. V. Fallani, J. R. Soc. Interface **15**, 20180514 (2018).

[27] J. Guillon, M. Chavez, F. Battiston, Y. Attal, V. L. Corte, M. T. de Schotten, B. Dubois, D. Schwartz, O. Colliot, and F. D. V. Fallani, Netw. Neurosci. **3**, 635 (2019).

[28] V. E. Piperigou, J. Stat. Plan. Infer. **139**, 3891 (2009).

[29] Y. Shang, Phys. Rev. E **101**, 042306 (2020).

[30] C. M. Schneider, A. A. Moreira, J. S. Andrade, Jr., S. Havlin, and H. J. Herrmann, Proc. Natl. Acad. Sci. USA **108**, 3838 (2011).

[31] S. Osat, F. Radicchi, and F. Papadopoulos, Phys. Rev. Res. **2**, 023176 (2020).

[32] M.-C. Corsi, M. Chavez, D. Schwartz, N. George, L. Hugueville, A. E. Kahn, S. Dupont, D. S. Bassett, and F. D. V. Fallani, J. Neural Eng. **18**, 056002 (2021).

[33] G. R. Kiss, C. Armstrong, R. Milroy, and J. Piper, in *The Computer and Literary Studies*, edited by A. J. Aitken, R. W. Bailey, and N. Hamilton-Smith (Edinburgh University Press, Edinburgh, 1973), pp. 153–165.

[34] S. Li and S. Wen, Complexity **2017**, 9781890 (2017).

[35] R. B. Nelsen, *An Introduction to Copulas*, 2nd ed. (Springer, New York, 2006).